

EFFECT OF FLUID FORCES ON ROTOR STABILITY OF  
CENTRIFUGAL COMPRESSORS AND PUMPS

Jørgen Colding-Jørgensen  
Technical University of Denmark

SUMMARY

In this paper a simple two-dimensional model for calculating the rotor-dynamic effects of the impeller force in centrifugal compressors and pumps is presented. It is based on potential flow theory with singularities. Equivalent stiffness and damping coefficients are calculated for a machine with a vaneless volute formed as a logarithmic spiral. It appears that for certain operating conditions, the impeller force has a destabilizing effect on the rotor. The order of magnitude of this effect can be determined from the stiffness and damping coefficients calculated. The paper is a brief review of the author's thesis (ref. 14), where more details of the calculation can be found.

SYMBOLS

|           |   |
|-----------|---|
| $A_{ij}$  | induced velocity in normal direction in point $i$ from singularity in point $j$ |
| $B$       | Busemann factor   |
| $B_{ij}$  | damping coefficient   |
| $b_{ij}$  | dimensionless damping coefficient   |
| $b_L$     | impeller width  |
| $b_0$     | diffuser width at inlet   |
| $b_2$     | diffuser width at outlet  |
| $c$       | absolute velocity of fluid at impeller outlet                                   |
| $c_i$     | induced velocity  |
| $D_L$     | impeller diameter   |
| $\bar{e}$ | eccentricity of rotor center  |
| $F_i$     | impeller force  |
| $f_i$     | dimensionless impeller force  |
| $K_{ij}$  | stiffness coefficient   |
| $k_{ij}$  | dimensionless stiffness coefficient   |
| $N$       | number of elements  |
| $\bar{n}$ | normal vector   |
| $Q$       | total volume flow in impeller   |

|            |  |
|------------|--|
| $Q_{opt}$  | optimum volume flow                                  |
| $Q_{rel}$  | total flow relative to optimum flow                  |
| $r_L$      | impeller radius                                      |
| $r_0$      | smallest radius of spiral                            |
| $U$        | tip velocity of impeller                             |
| $v_\infty$ | velocity from vortex source                          |
| $\alpha_0$ | angle between flow velocity and peripheral direction |
| $\beta$    | blade angle of impeller                              |
| $\Gamma$   | total circulation of impeller flow                   |
| $\gamma$   | vortex strength per unit length                      |
| $\rho$     | density of fluid                                     |

### INTRODUCTION

The linearized governing equation for self-sustained lateral vibration of a rotor can be written

$$\underline{M}\ddot{\underline{q}} + \underline{C}\dot{\underline{q}} + \underline{K}\underline{q} = \underline{0} \quad (1)$$

in the absence of external forces. The vector  $\underline{q}$  represents the generalized coordinates of the system,  $\underline{M}$  is the mass matrix,  $\underline{C}$  the damping matrix, and  $\underline{K}$  the stiffness matrix. The stability of the system is determined by the solution to the equation

$$\det(\underline{M}\lambda^2 + \underline{C}\lambda + \underline{K}) = 0 \quad (2)$$

where  $\lambda = \alpha + i\beta$  and  $\underline{q} = \underline{A}e^{\lambda t}$ . If  $\alpha > 0$ , the system is unstable. Apart from elastic forces and inertia forces due to the deflection of the rotor itself, these matrices also depend on forces from bearings and seals. Furthermore in turbomachinery, forces from the working fluid acting on the rotor may affect the matrices and consequently alter the stability of the rotor (ref. 10).

In centrifugal pumps and compressors the working fluid exerts a force on the rotor caused by diffuser/impeller interaction, as shown experimentally and theoretically by different authors (refs. 1 to 9). As indicated by Domm and Hergt (ref. 2) and Hergt and Krieger (ref. 8), this force depends on the eccentricity of the rotor. In the literature this force is often called the radial force, but this term is a bit misleading in a rotordynamic sense since the force also has a tangential component. Therefore in this paper it will be called the impeller force.

In this paper a method is presented for calculating the impeller force, its dependency on the rotor eccentricity, and the force's associated stiffness coefficients. Furthermore it is shown that the impeller force also depends on the velocity of the rotor center. This gives rise to equivalent damping coefficients, which are also calculated. For simplicity the analysis is restricted to centrifugal pumps with a vaneless volute but can be extended to any

kind of diffuser, as long as neither losses associated with friction and three-dimensional flow nor compressibility seriously affects the pressure-distribution around the impeller. The calculated stiffness and damping coefficients represent the contribution to the stiffness and damping matrices  $\underline{K}$  and  $\underline{C}$  from the impeller force and thus permit one to determine the influence of the impeller force on rotor stability and synchronous response.

#### PHYSICAL MODEL

This model of a centrifugal pump or compressor stage with a vaneless volute is founded on the concept of Csanady (ref. 1). It is based on a two-dimensional representation of the diffuser and a representation of the impeller by an equivalent vortex source concentrated in a single point, as shown in figure 1.

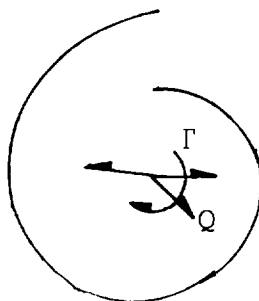


Figure 1

The flow is considered a potential flow field with the singularity  $Q, \Gamma$ .

The vortex-source point coincides with the rotor center, and it may have any eccentricity and velocity in a coordinate system fixed to the diffuser. The source strength and vortex strength  $Q$  and  $\Gamma$  are related to parameters of the impeller as shown later.

#### CALCULATION OF FLOW FIELD

The flow field is calculated by a singularity method, that is, a method based on the replacement of the diffuser contour by a distribution of vortices and/or sources. The method used was developed by Hess (ref. 11). The diffuser contour is considered as a series of small linear segments. Each segment is covered by a vortex distribution of uniform strength. The vortex strength varies from segment to segment. The normal component of the flow field on the contour must be zero. If we have  $N$  linear segments, we have  $N$  vortex strengths, and hence we can satisfy the condition in  $N$  points. These points are chosen as the  $N$  midpoints of the segments.

In a potential flow field with potential singularities the law of superposition is valid; that is, the velocity in any point is the sum of the velocities induced by all singularities in the field. Thus the kinematic conditions give

$$\sum_{j=1}^N A_{ij} \gamma_j = -\underline{V}_{\infty i} \cdot \underline{n}_i \quad (3)$$

where  $\underline{V}_{\infty i}$  is the velocity at the midpoint at section  $i$  produced by the impeller flow (through the vortex source  $\Gamma, Q$  representation) with the impeller assigned some given eccentricity and velocity. The coefficients  $A_{ij}$  are evaluated as the normal velocity components induced in point  $i$  by a unit vortex strength along line segment  $j$ . The term  $\gamma_j$  is the unknown vortex strength per unit length of line segment  $j$ ;  $\underline{V}_{\infty i}$  is the velocity induced by the vortex source  $\Gamma, Q$  representing the impeller for a given eccentricity and velocity of the vortex source.

The solution of equation (3) gives the values of  $\gamma_j$  for all  $j = 1, N$ . After solution of equation (3), all the singularities in the flow field are determined, and thus the velocity in any point in the plane can be calculated. The development of the coefficients  $A_{ij}$  and  $\underline{V}_{\infty i} \cdot \underline{n}_i$  is shown in appendix A for any rotor-center eccentricity and velocity. The method presented is valid for a vaneless volute with the rotor center coinciding with the spiral center for zero eccentricity. It could be developed for any diffuser geometry as long as the pressure distribution around the impeller is satisfactorily calculated by means of potential theory. Equation (3) will normally contain a large number of linear equations - from 100 to several hundreds - and the coefficients of the system are generally different from zero.

#### DETERMINATION OF $Q$ AND $\Gamma$ FROM MACHINE DATA

Figure 2 illustrates the velocity vectors of the flow at the exit of the impeller. With Csanady's nomenclature (ref. 1) the variables of this figure are defined as follows:

- B Busemann slip factor, tabulated by Wislicenus (ref. 12) for different impellers; depends on blade angle and number of blades
- $\beta$  blade angle of impeller
- U tip velocity of rotor
- C absolute velocity of fluid at outlet

The total volume flow is

$$Q = 2\pi r_L b_L \sin \alpha_0 C \quad (4)$$

where  $r_L$  and  $b_L$  are the radius and the width of the impeller, respectively. From figure 2

$$C(\cos \alpha_0 + \sin \alpha_0) \cot \beta = UB \quad (5)$$

Combining equations (4) and (5) yields

$$Q = UB 2\pi r_L b_L / (\cot \alpha_0 + \cot \beta) \quad (6)$$

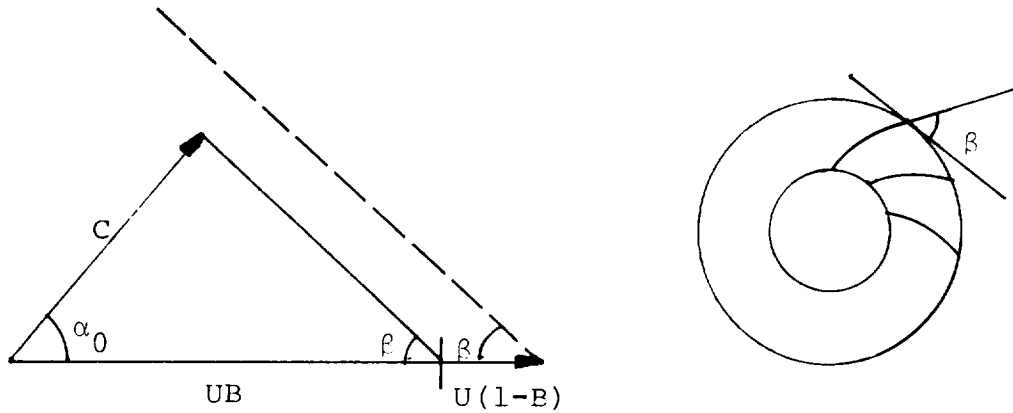


Figure 2

Furthermore

$$Q = \tan \alpha_0 \cdot \Gamma \quad (7)$$

because  $\alpha_0$  is the angle between the flow and the peripheral direction at the outlet. The optimum efficiency with a spiral-formed volute with spiral angle  $\lambda$  is obtained when

$$90^\circ - \lambda = \alpha_0$$

at the volume flow  $Q_{opt}$ , according to Csanady (ref. 1). From equation (6) we obtain

$$Q_{rel} = Q/Q_{opt} = \frac{\tan \alpha_0 (\tan \beta \tan \lambda + 1)}{(\tan \beta + \tan \alpha_0)} \quad (8)$$

#### CALCULATION OF IMPELLER FORCE

The force per unit width on a body with circulation  $\Gamma$  in the presence of a source  $Q$  in a parallel stream with the velocity  $\underline{c}$  is, according to the theorems of Joukowski and Lagally (in ref. 13)

$$\underline{F} = \rho (\underline{c}Q + \hat{c}\Gamma) \quad (9)$$

where  $\rho$  is the density of the fluid. If we consider the velocity induced by the singularity distribution on the diffuser contour to be a parallel stream in the calculation of the impeller force, the impeller force is obtained by inserting equations (6) and (7) into equation (9) to yield

$$\underline{F}_i = \frac{UB2\pi r_L b_L}{1 + \tan \alpha_0 / \tan \beta} (\hat{c}_i + \tan \alpha_0 \underline{c}_i) \quad (10)$$

In this equation,  $\underline{c}_j$  is the velocity induced in the rotor center by the contour singularity distribution, as determined from equation (3). The solution procedure for  $\underline{c}_j$  for any rotor-center eccentricity and velocity is carried out in appendix B for a vaneless volute formed as a logarithmic spiral, whose center coincides with the rotor center for zero eccentricity. The procedure requires the vortex distribution solution  $\gamma_j$  from equation (3). This could be done for any diffuser geometry.

CALCULATION OF EQUIVALENT STIFFNESS  
AND DAMPING COEFFICIENTS

The impeller force can be calculated for any eccentricity and velocity of the rotor center as shown on the previous pages. The force is now calculated for different combinations of eccentricity and velocity of the rotor center in the x- and y-directions of figure 3.

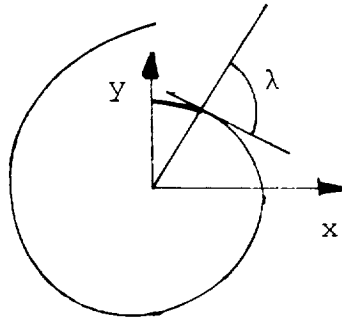


Figure 3

The values of the force can then be tabulated or stored in the computer, and the equivalent stiffness and damping coefficients are calculated as the following numerical derivations:

$$\left. \begin{aligned} K_{ij} &= -\Delta F_i / \Delta e_j \\ B_{ij} &= -\Delta F_i / \Delta v_j \end{aligned} \right\} (i=1,2; j=1,2) \quad (11)$$

where the index 1 corresponds to the x-direction, and the index 2 corresponds to the y-direction.

RESULTS

On the following pages some calculation results are shown for a given impeller with different volute-spiral angles. The force and stiffness and damping coefficients are presented in the following forms:

$$f_i = F_i / (U^2 \rho / 2 b_L D_L)$$

$$b_{ij} = B_{ij} / (U \rho / 2 b_L D_L) \quad (12)$$

$$k_{ij} = K_{ij} / (U^2 \rho b_L)$$

with  $D_L = 2r_L$ . The impeller has  $B = 0.8$ ,  $\beta = 22.5^\circ$ . Furthermore  $b_0/b_2 = 0.7$  and  $r_L/r_0 = 0.9$ , where  $r_0$  is the smallest radius of the spiral. The calculation is carried out for  $\lambda = 83^\circ$ ,  $86^\circ$ , and  $88^\circ$ . The relative flow  $Q_{rel}$  is determined from equation (8).

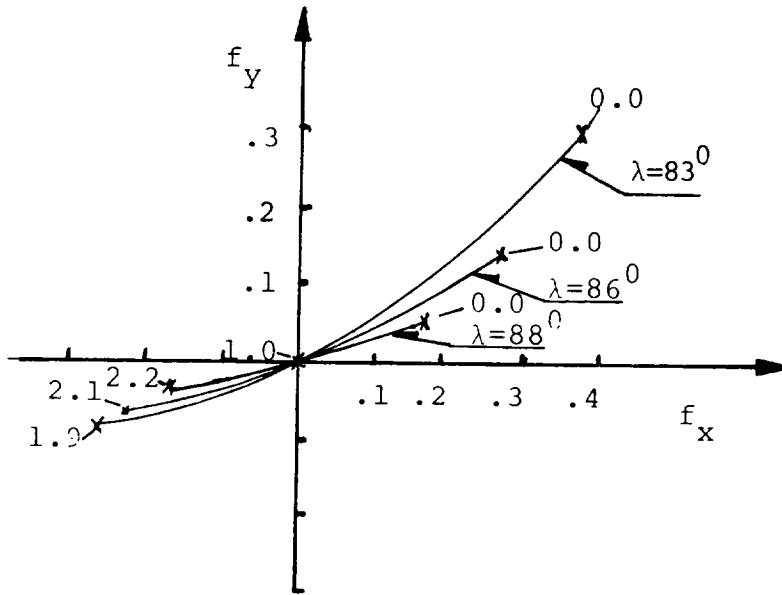


Figure 4

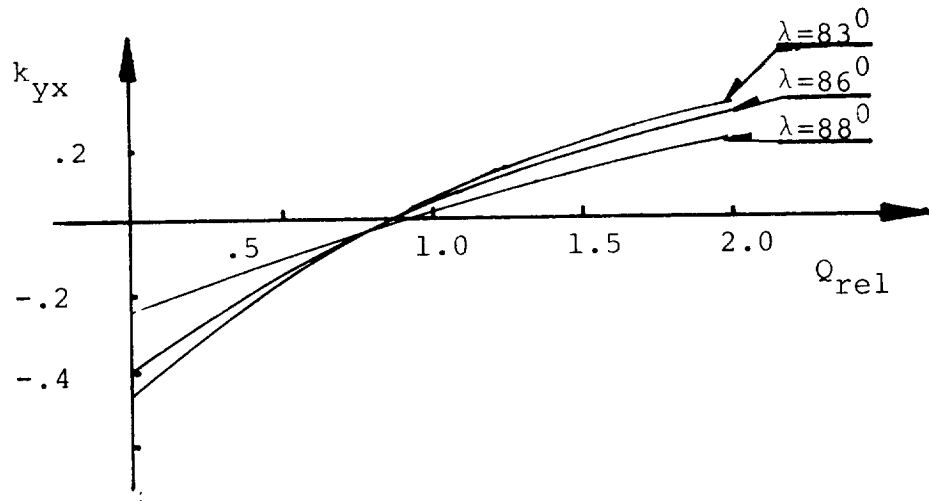


Figure 5

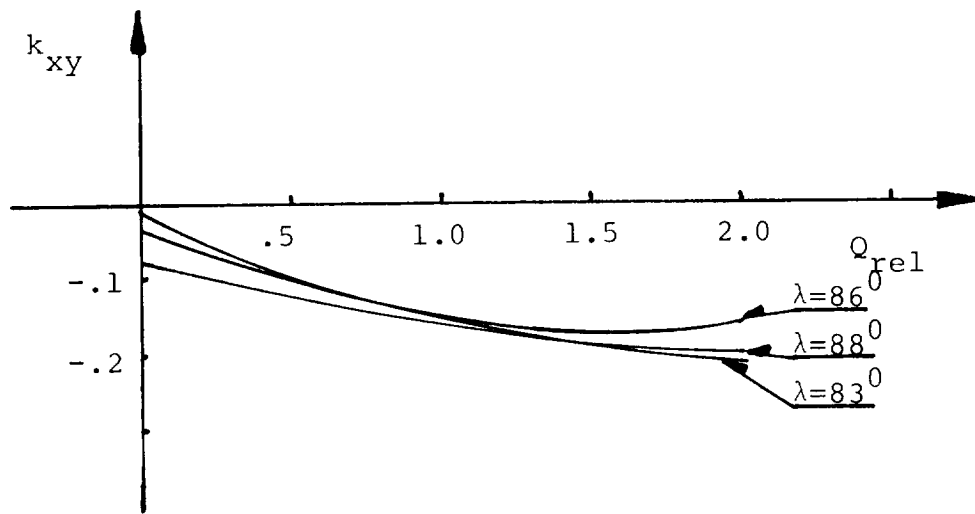


Figure 6

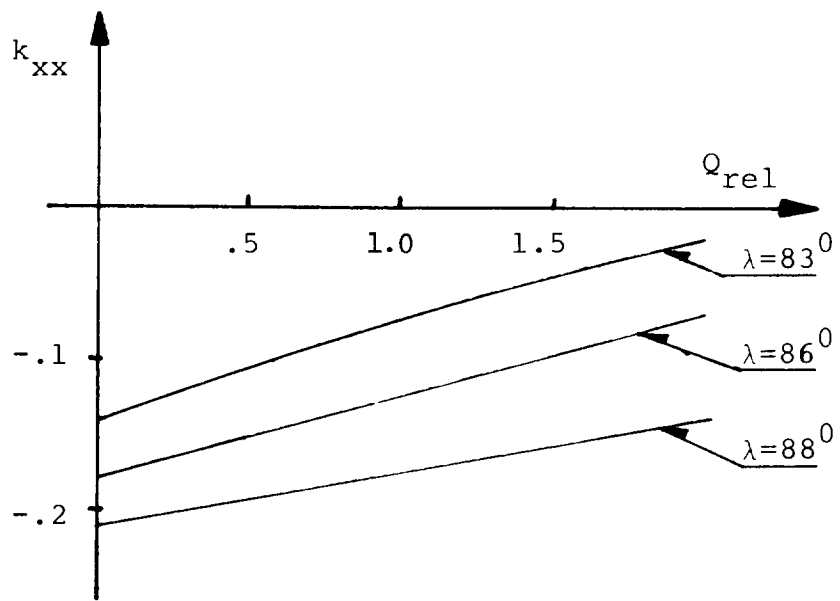


Figure 7

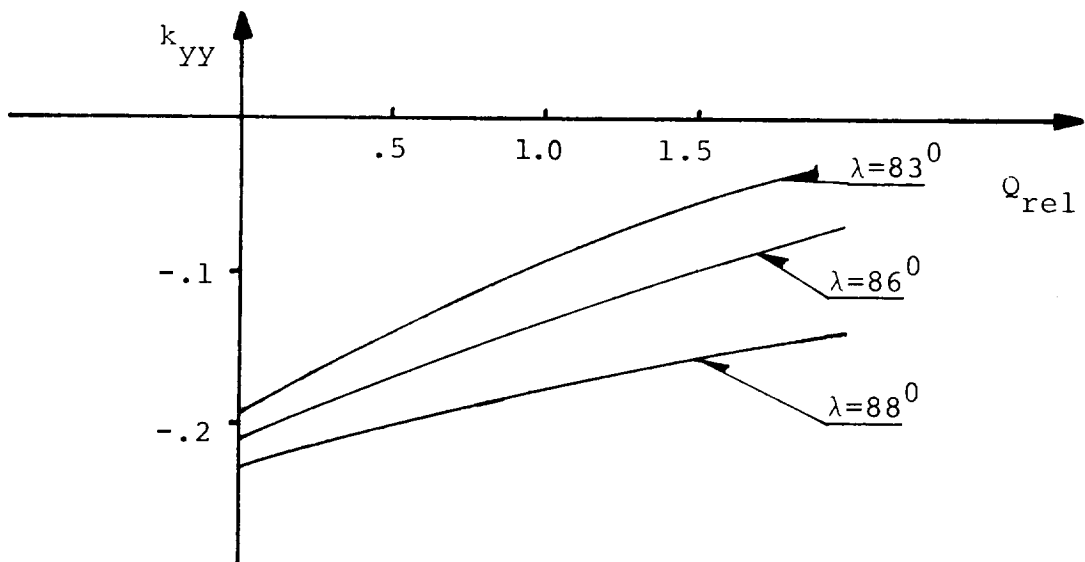


Figure 8

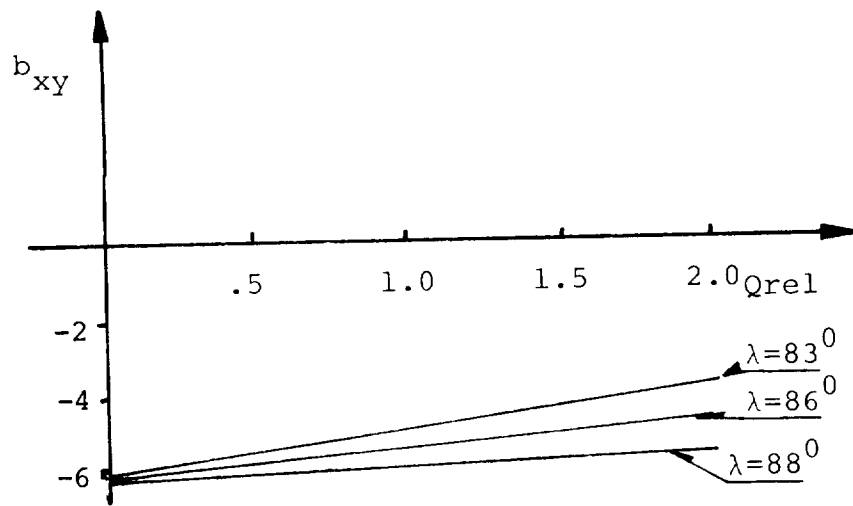


Figure 9

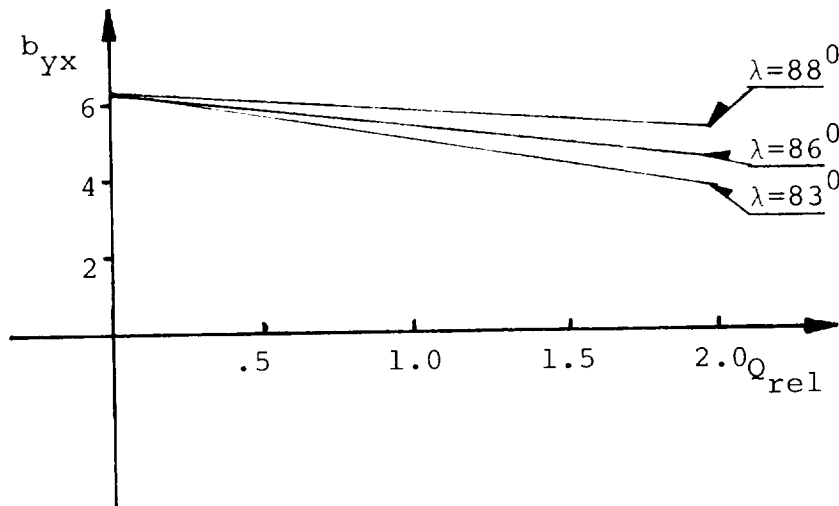


Figure 10

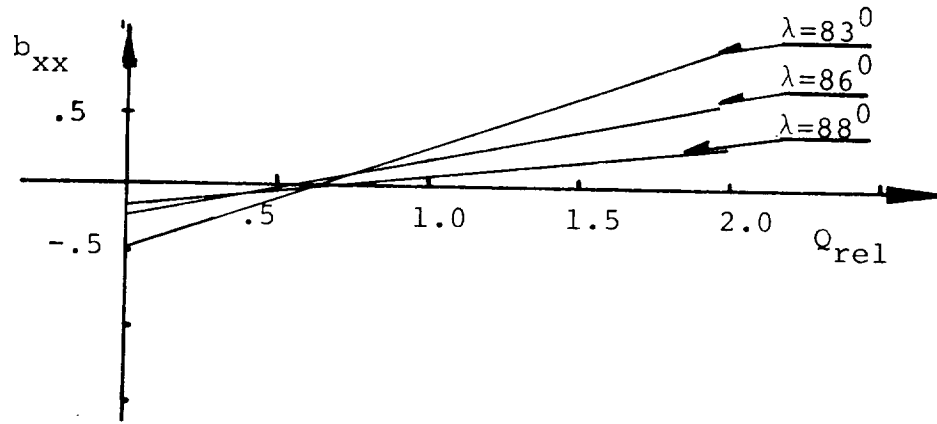


Figure 11

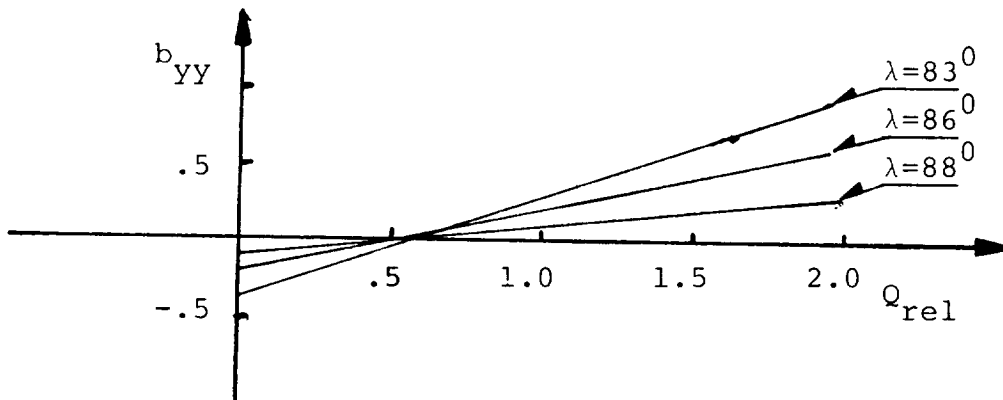


Figure 12

## DISCUSSION

From figures 5 and 6 we see that for certain relative flows the cross-coupling stiffness coefficients  $K_{XY}$  and  $K_{YX}$  have opposite signs. This means that the impeller force has a destabilizing effect on the rotor. Furthermore the damping coefficients  $B_{XX}$  and  $B_{YY}$  become negative for certain values of the relative flows (figs. 11 and 12). This negative damping is highly destabilizing. For the cross-coupling damping coefficients  $B_{XY}$  and  $B_{YX}$ , we have almost exactly  $B_{XY} = -B_{YX}$  (figs. 9 and 10), and these coefficients are 4 to 10 times larger than  $B_{XX}$  and  $B_{YY}$ . This means that the rotor is subject to relatively large gyroscopic forces. These forces would tend to stabilize the rotor.

The spiral angle  $\lambda$  is a significant design parameter, as seen in figures 4 to 12. For increasing  $\lambda$  the impeller force decreases in magnitude, the stiffness coefficients increase in magnitude,  $B_{XX}$  and  $B_{YY}$  decrease in magnitude, and  $B_{YX}$  and  $B_{XY}$  increase in magnitude. The interval where the destabilizing effects are absent is moved to the right on the  $Q_{rel}$  -axis for increasing  $\lambda$  as seen from figures 5, 6, 9, and 10. The effects of impeller design parameters are not investigated in this paper. This effect could, if wished, be calculated by equation (8).

The only relevant measurements reported in the literature are those determining the impeller force as a function of the relative flow (refs. 2 to 5 and 9). There is qualitative agreement between the reported values of the magnitude of the impeller force and the present calculations. As for the direction of the force there is a large scatter in the results reported in the literature, and the results of this paper consequently only agree with some of these results. No direct measurements of stiffness and damping coefficients are reported in the literature. Experimental determination of stiffness and damping coefficients associated with the impeller force must be made before a comparison of calculated and measured values is possible.

APPENDIX A

CALCULATION OF INFLUENCE COEFFICIENTS  $A_{ij}$  AND  $V_{\infty i n_i}$  FOR A  
VANELESS VOLUTE FORMED AS LOGARITHMIC SPIRAL

For this purpose we have to use some basic formulas from potential-flow theory. The velocity induced in a point  $(x,y)$  by an infinitely long line source in  $(0,0)$  is

$$\begin{pmatrix} u \\ v \end{pmatrix}_Q = Q/2 \ 1/(x^2 + y^2) \begin{pmatrix} x \\ y \end{pmatrix} \quad (13)$$

where  $Q$  is the source strength. For a vortex line of strength  $\Gamma$ , the corresponding velocity is

$$\begin{pmatrix} u \\ v \end{pmatrix} = \Gamma/2 \ 1/(x^2 + y^2) \begin{pmatrix} y \\ -x \end{pmatrix} \quad (14)$$

If we have a line segment placed as in figure 13, covered with a constant vortex strength of unity, an integration over the segment gives the following velocity induced by the line segment in point  $(x,y)$  (ref. 11):

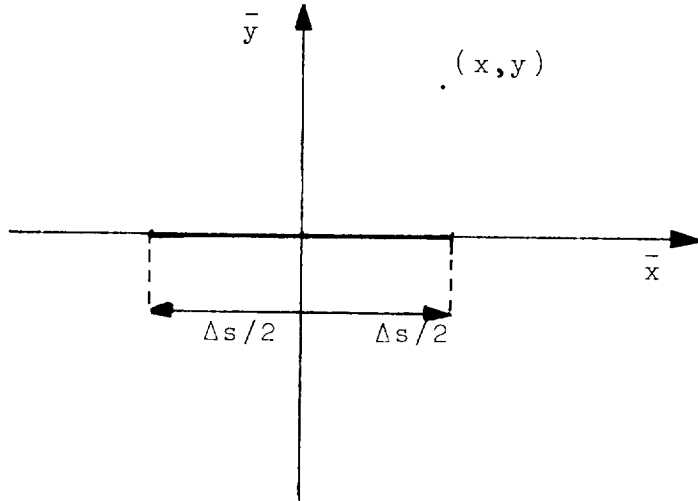


Figure 13

$$\left. \begin{aligned} v_x &= 1/2\pi \left[ \arctan \left( \frac{x + \Delta s/2}{y} \right) - \arctan \left( \frac{x - \Delta s/2}{y} \right) \right] \\ v_y &= -1/4\pi \ln \left[ \frac{(x + \Delta s/2)^2 + y^2}{(x - \Delta s/2)^2 + y^2} \right] \end{aligned} \right\} \quad (15)$$

where  $V_y \rightarrow 0$  and  $V_x \rightarrow 1/2$  for  $x = 0, y \rightarrow 0$ . Consider the logarithmic spiral of figure 14.

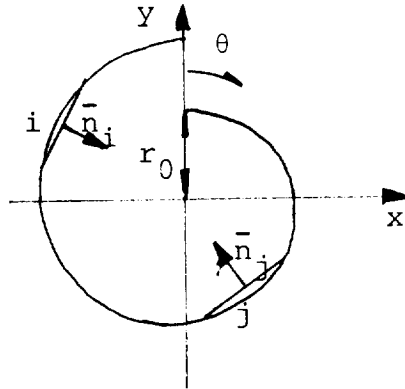


Figure 14

Take  $\theta_i$  and  $\theta_j$  as the values of the angle  $\theta$  for the position vector of the midpoint of the line segment  $i$  and  $j$ . We have from figure 14

$$\underline{n}_i = \begin{bmatrix} \cos(\theta_i + \lambda) \\ -\sin(\theta_i + \lambda) \end{bmatrix} \quad (16)$$

$$\begin{pmatrix} x \\ y \end{pmatrix} = r_0 e^{\theta_j / \tan \lambda} \begin{pmatrix} \sin \theta_j \\ \cos \theta_j \end{pmatrix} + \begin{bmatrix} -\sin(\theta_j + \lambda) & \cos(\theta_j + \lambda) \\ -\cos(\theta_j + \lambda) & -\sin(\theta_j + \lambda) \end{bmatrix} \begin{pmatrix} x'_j \\ y'_j \end{pmatrix} \quad (17)$$

$$\begin{pmatrix} x'_j \\ y'_j \end{pmatrix} = \begin{bmatrix} -\sin(\theta_j + \lambda) & -\cos(\theta_j + \lambda) \\ \cos(\theta_j + \lambda) & -\sin(\theta_j + \lambda) \end{bmatrix} \begin{pmatrix} x - r_0 e^{\theta_j / \tan \lambda} \sin \theta_j \\ y - r_0 e^{\theta_j / \tan \lambda} \cos \theta_j \end{pmatrix} \quad (18)$$

These coordinate transformations are necessary for the calculation of the induced velocities from the vortex distribution. Furthermore we have for the induced velocities in the different coordinate systems

$$\begin{pmatrix} v_{xin} \\ v_{yin} \end{pmatrix} = \begin{bmatrix} -\sin(\theta_j + \lambda) & \cos(\theta_j + \lambda) \\ -\cos(\theta_j + \lambda) & -\sin(\theta_j + \lambda) \end{bmatrix} \begin{pmatrix} v'_{x_j in} \\ v'_{y_j in} \end{pmatrix} \quad (19)$$

If the point  $(x_i, y_i)$  is the midpoint of line segment  $i$ , we have

$$\begin{pmatrix} x_i \\ y_i \end{pmatrix} = r_0 e^{\theta_i / \tan \lambda} \begin{pmatrix} \sin \theta_i \\ \cos \theta_i \end{pmatrix} \quad (20)$$

Hence, by using the coordinate transformation (18), the coordinates of point  $(x_i, y_i)$  in reference system  $(x'_j, y'_j)$  are

$$\begin{pmatrix} x'_{ij} \\ y'_{ij} \end{pmatrix} = r_0 \begin{bmatrix} -e^{\theta_i/\tan \lambda} \cos(\lambda + \theta_j - \theta_i) + e^{\theta_j/\tan \lambda} \cos \lambda \\ -e^{\theta_i/\tan \lambda} \sin(\lambda + \theta_j - \theta_i) + e^{\theta_j/\tan \lambda} \sin \lambda \end{bmatrix} \quad (21)$$

From equations (16), (21) and (15), we get  $A_{ij}$ , the normal velocity induced in point  $i$  from line segment  $j$

$$A_{ij} = 0 \quad \text{for } i = j$$

$$A_{ij} = \frac{1}{4\pi} \left\{ -\sin(\theta_i - \theta_j) 2 \left[ \arctan \left( \frac{x'_{ij} + \Delta s/2}{y'_{ij}} \right) - \arctan \left( \frac{x'_{ij} - \Delta s/2}{y'_{ij}} \right) \right] \right. \\ \left. + \cos(\theta_i - \theta_j) \ln \left( \frac{(x'_{ij} + \Delta s/2)^2 + y'^2_{ij}}{(x'_{ij} - \Delta s/2)^2 + y'^2_{ij}} \right) \right\} \quad \text{for } i \neq j \quad (22)$$

In addition, from equations (13), (14), (7), and (20), we obtain

$$\underline{n}_i V_{\infty i} = \begin{bmatrix} -\cos(\theta_i + \lambda) \\ \sin(\theta_i + \lambda) \end{bmatrix} \left[ \begin{pmatrix} v_x \\ v_y \end{pmatrix} + Q/2\pi \underline{r}_i^2 (\underline{r}_i - \cot \alpha_0 \hat{r}_i) \right]$$

$$\text{with } \underline{r}_i = \begin{pmatrix} x_i \\ y_i \end{pmatrix} - \begin{pmatrix} e_x \\ e_y \end{pmatrix}$$

This is the induced velocity in the normal direction in point  $i$  from the vortex source  $(Q, \Gamma)$  in the impeller center with eccentricity  $(e_x, e_y)$  and velocity  $(v_x, v_y)$ . For this geometry a correction is required because the volute does not have a constant width. Domm and Hergt (ref. 2) use the correction factor  $b_0/b_2$ , where  $b_0$  is the width at inlet and  $b_2$  the width at outlet of the volute, so the final result is

$$\underline{n}_i V_{\infty i} = b_0/b_2 \begin{bmatrix} -\cos(\theta_i + \lambda) \\ \sin(\theta_i + \lambda) \end{bmatrix} \left[ \begin{pmatrix} v_x \\ v_y \end{pmatrix} + Q/2\pi \underline{r}_i^2 (\underline{r}_i - \cot \alpha_0 \hat{r}_i) \right] \quad (23)$$

APPENDIX B

CALCULATION OF INDUCED VELOCITY IN ROTOR CENTER

From equations (15), (18), and (19), we can calculate the induced velocity contribution for each line segment in any point in the plane. If we calculate these contributions in the rotor center, the total induced velocity in the rotor center is the following sum from all N line segments of the volute contour:

$$\begin{pmatrix} v_x \\ v_y \end{pmatrix}_{\text{center}} = \sum_{j=1}^N \begin{pmatrix} v_{x_j} \\ v_{y_j} \end{pmatrix}_{\text{center}}$$

But the rotor center has the velocity  $(v_x, v_y)$ , so the induced velocity is

$$\underline{c}_i = \sum_{j=1}^N \begin{pmatrix} v_{x_j} \\ v_{y_j} \end{pmatrix}_{\text{center}} - \begin{pmatrix} v_x \\ v_y \end{pmatrix} \quad (24)$$

## REFERENCES

1. Csanady, G. T.: Radial Forces in a Pump Impeller Caused by Volute Casing. J. Eng. Power, Oct. 1962, p. 337.
2. Domm, U.; and Hergt, P.: Radial Forces on Impeller of Volute Casing Pumps, Flow Research on Blading. L. S. Dzung, ed., Elsevier, 1971, p. 305.
3. Agnostelli, A.; Nobles, D.; and Mockridge, C. R.: An Experimental Investigation of Radial Thrust in Centrifugal Pumps. J. Eng. Power, April 1960, p. 120.
4. Biheller, H. J.: Radial Force on the Impeller of Centrifugal Pumps with Volute, Semivolute, and Concentric Casings. J. Eng. Power, July 1965, p. 319.
5. Iversen, H. W.; Rolling, R. E.; and Carlson, J. J.: Volute Pressure Distribution, Radial Force on the Impeller, and Volute Mixing Losses of a Radial Flow Centrifugal Pump. J. Eng. Power, April 1960, p. 136.
6. Black, H. F.: Lateral Stability and Vibration of High Speed Centrifugal Pumps. Symp. on Dynamics of Rotors, IUTAM, Dept. of Solid Mech., Tech. Univ. Denmark, 1974.
7. Grein, H., and Bachmann, P.: Radial Forces on Hydraulic Turbomachinery, Part 1. Sulzer Technical Review 1, 1975, p. 37.
8. Hergt, P.; and Krieger, P.: Radial Forces in Centrifugal Pumps with Guide Vanes. Proceedings of the Institution of Mechanical Engineers 1969-70, vol. 184, pt. 3N, p. 101.
9. Grotrian, J. Meir: Untersuchungen der Radialkraft auf das Laufrad einer Kreiselpumpe bei Verschiedenen Spiralgehäuse-formen, VDI-Bericht, no. 193, 1973.
10. Black, H. F.: Calculation of Forced Whirling and Stability of Centrifugal Pump Rotor Systems. J. Eng. Industry, Aug. 1974, p. 107.
11. Hess, J. L.: Numerical Solution of Inviscid Subsonic Flows, Von Karman Inst. for Fluid Dynamics, Lecture Series 34, March 1971.
12. Wislicenus, G. F.: Fluid Mechanics of Turbomachinery, McGraw-Hill Book Co., Inc., New York, 1947.
13. Robertson, J. M.: Hydrodynamics in Theory and Application, Prentice Hall, 1965.
14. Colding-Jørgensen, J.: Fluidkræfternes Indvirkning på Stabiliteten af Centrifugalpumper og Kompressorer. Dept. of Machine Design, Tech. Univ. Denmark, 1979.

